Published September 28, 2009

INTS3 controls the hSSB1-mediated DNA damage response

Jeffrey R. Skaar,[2] Derek J. Richard,[3] Anita Saraf,[4] Alfredo Toschi,[2] Emma Bolderson,[3] Laurence Florens,[4] Michael P. Washburn,[4] Kum Kum Khanna,[3] and Michele Pagano[1,2]

[1]Howard Hughes Medical Institute and [2]Department of Pathology, New York University Cancer Institute, New York University School of Medicine, New York, NY 10016
[3]Queensland Institute of Medical Research, Herston, Queensland 4006, Australia
[4]Stowers Institute for Medical Research, Kansas City, MO 64110

Human SSB1 (single-stranded binding protein 1 [hSSB1]) was recently identified as a part of the ataxia telangiectasia mutated (ATM) signaling pathway. To investigate hSSB1 function, we performed tandem affinity purifications of hSSB1 mutants mimicking the unphosphorylated and ATM-phosphorylated states. Both hSSB1 mutants copurified a subset of Integrator complex subunits and the uncharacterized protein LOC58493/c9orf80 (henceforth minute INTS3/hSSB-associated element [MISE]). The INTS3–MISE–hSSB1 complex plays a key role in ATM activation and RAD51 recruitment to DNA damage foci during the response to genotoxic stresses. These effects on the DNA damage response are caused by the control of hSSB1 transcription via INTS3, demonstrating a new network controlling hSSB1 function.

Introduction

In response to threats to genome integrity, cells have evolved elaborate pathways for sensing and repairing DNA damage. The DNA damage response infiltrates all aspects of cell physiology, including basic processes such as transcription. The involvement of components of the transcriptional machinery with DNA damage pathways has a long history, with members of the RNA polymerase II–associated basal transcription machinery impacting both nucleotide excision repair (Lainé and Egly, 2006) and double-strand break responses (Buchmann et al., 2004; Derheimer et al., 2007).

The Integrator complex was initially characterized as an RNA polymerase II C-terminal domain–binding factor involved in the 3′ processing of small nuclear RNAs (snRNAs; Baillat et al., 2005). The Integrator complex contains at least 12 subunits whose individual contributions to snRNA processing or broader cellular functions remain largely uncharacterized. The snRNA processing activity is provided by a β-lactamase domain in INTS11, which shows homology to the cleavage-specific polyadenylation factor 73 (Baillat et al., 2005). INTS1 and -5 are also required for snRNA processing (Dominski et al., 2005; Tao et al., 2009), but the functions of other INTS proteins remain largely unexplored. INTS6 was initially described as a tumor suppressor (Wieland et al., 1999), and INTS1 is required for early embryonic development (Hata and Nakayama, 2007). Whether these functions are Integrator dependent has not been addressed, and neither Integrator nor its individual subunits have been linked to DNA damage responses.

The ataxia telangiectasia mutated (ATM) kinase is a master regulator of the response to DNA double-strand breaks, phosphorylating multiple targets to institute cell cycle arrest (e.g., phosphorylation of p53 and CHK2) and coordinate the repair of DNA damage (e.g., phosphorylation of BRCA1, H2AX, and the MRN [Mre11–Rad50–Nbs1] complex; Lavin, 2007). Recently, the oligonucleotide/oligosaccharide-binding (OB) fold protein human SSB1 (single-stranded binding protein 1 [hSSB1]; OBFC2B/NABP2) was identified as a key player in the ATM-mediated response to DNA double-strand breaks (Kang et al., 2006; Richard et al., 2008), with ATM-mediated phosphorylation of Thr117 stabilizing hSSB1. Although hSSB1 is an ATM target, hSSB1 function is required for activation of ATM kinase activity after DNA damage. hSSB1 localizes directly to

Correspondence to Michele Pagano: michele.pagano@nyumc.org

Abbreviations used in this paper: ATM, ataxia telangiectasia mutated; HR, homologous recombination; MISE, minute INTS3/hSSB-associated element; NHF, normal human fibroblast; NSAF, normalized spectral abundance factor; OB, oligonucleotide/oligosaccharide binding; snRNA, small nuclear RNA.

Supplemental Material can be found at:
http://jcb.rupress.org/content/suppl/2009/09/27/jcb.200907026.DC1.html

The Rockefeller University Press $30.00
J. Cell Biol. Vol. 187 No. 1 25–32
www.jcb.org/cgi/doi/10.1083/jcb.200907026

Published September 28, 2009

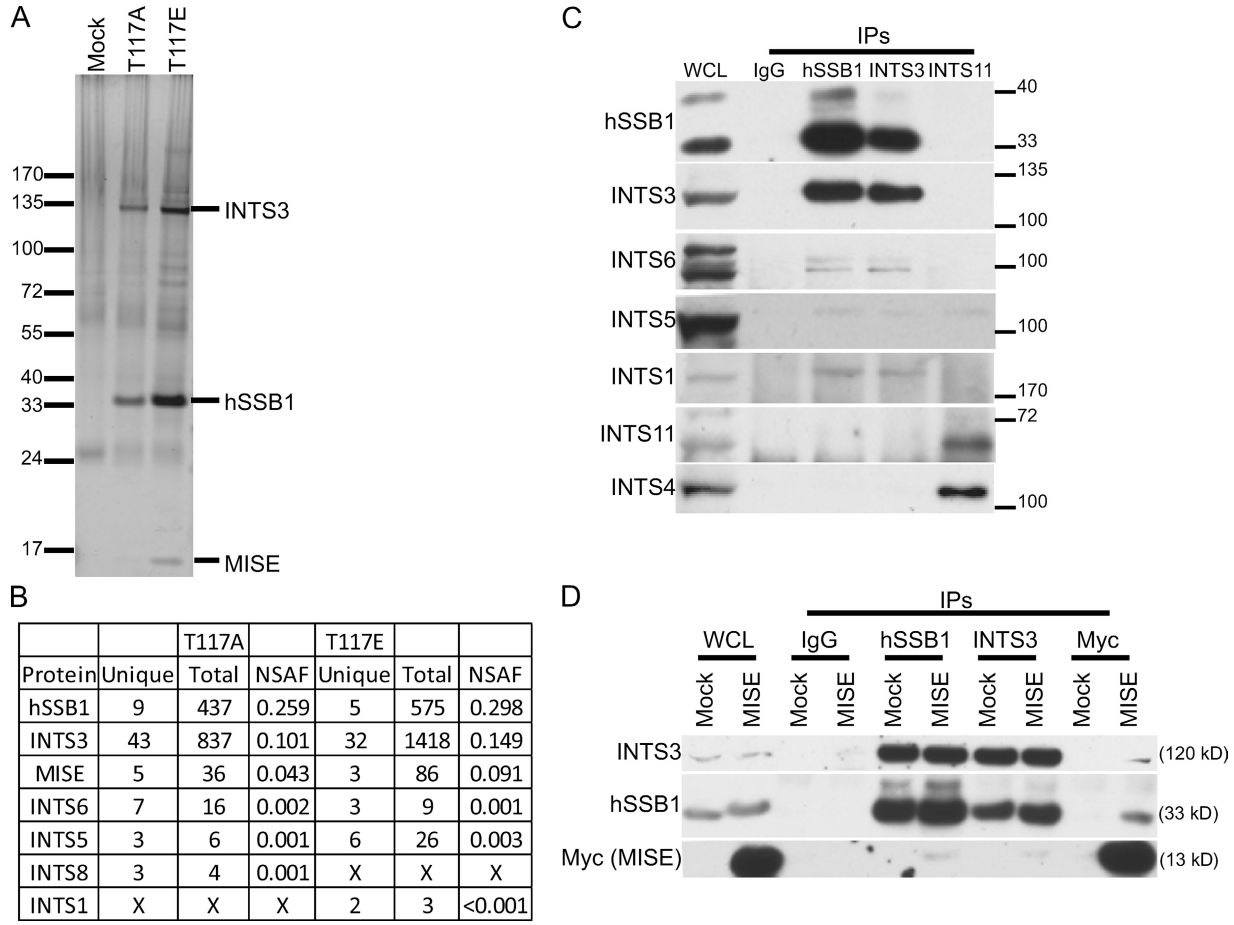

B

		T117A		T117E		
Protein	Unique	Total	NSAF	Unique	Total	NSAF
hSSB1	9	437	0.259	5	575	0.298
INTS3	43	837	0.101	32	1418	0.149
MISE	5	36	0.043	3	86	0.091
INTS6	7	16	0.002	3	9	0.001
INTS5	3	6	0.001	6	26	0.003
INTS8	3	4	0.001	X	X	X
INTS1	X	X	X	2	3	<0.001

Figure 1. **hSSB1 binds INTS3 and MISE.** (A) HEK293T cells transfected with Flag-HA–hSSB1 T117A or Flag-HA–hSSB1 T117E were harvested for tandem affinity purification. 5% of the Flag-HA–hSSB1 T117A, Flag-HA–hSBB1 T117E, and control purifications was subjected to SDS-PAGE and silver staining. (B) MudPIT analysis of the purifications in A, listing unique peptides, total peptides, and NSAFs for the indicated proteins. (C) U-2 OS cell lysates were immunoprecipitated for the indicated proteins, separated by SDS-PAGE, and Western blotted as indicated. (A and C) Molecular mass is indicated in kilodaltons. (D) HEK293T cells were mock transfected or transfected with Myc-MISE. 48 h after transfection, cells were harvested, and lysates were immunoprecipitated as indicated, before SDS-PAGE and Western blotting as indicated. IP, immunoprecipitation; WCL, whole cell lysate.

double-strand breaks and stimulates strand invasion by RAD51, which is consistent with a function in DNA repair by homologous recombination (HR). Consequently, the loss of hSSB1 results in radiosensitivity and genomic instability.

Despite the identification of hSSB1 as a member of the ATM pathway, the molecular mechanisms controlling hSSB1 functions remain to be elucidated. In this study, we identify a novel hSSB1-containing complex that is required for an effective response to DNA damage.

Results and discussion

hSSB1 binds a novel INTS3-containing complex

To investigate the function of hSSB1, hSSB1 mutants mimicking the constitutively unphosphorylated (T117A) or phosphorylated (T117E) protein were tandem affinity purified from HEK293T cells (Fig. 1 A; Nakatani and Ogryzko, 2003). Consistent with previously reported stability differences (Richard et al., 2008), less T117A was purified compared with T117E. However, MudPIT analysis (Washburn et al., 2001) revealed little difference in the associated proteins of hSSB1 T117A and T117E. Both proteins associated with a subset of members of the Integrator complex and LOC58493/c9orf80, a novel, uncharacterized 11-kD protein which we have named minute INTS3/hSSB-associated element (MISE; Fig. 1 B) to reflect its small size and association with INTS3 and hSSB1. The association of the hSSB1 mutants with INTS3 and MISE was particularly robust, as demonstrated by both silver staining and their normalized spectral abundance factors (NSAFs; Zybailov et al., 2007). Although large amounts of INTS3 were found via MudPIT analysis, only a few peptides were found for other members of the Integrator complex, including (in order of NSAFs) INTS6, -5, -8, and -1, and no peptides were found for INTS11, the catalytic subunit of the Integrator complex which is required for snRNA processing. The combination of the large NSAF values for hSSB1, INTS3, and MISE, in conjunction with the absence of the INTS11, suggested that the hSSB1–INTS3 complex is unique and separate from the previously described Integrator complex (Baillat et al., 2005). Therefore, we will refer to this complex as the INTS3–MISE–hSSB1 (IMS1) complex.

Published September 28, 2009

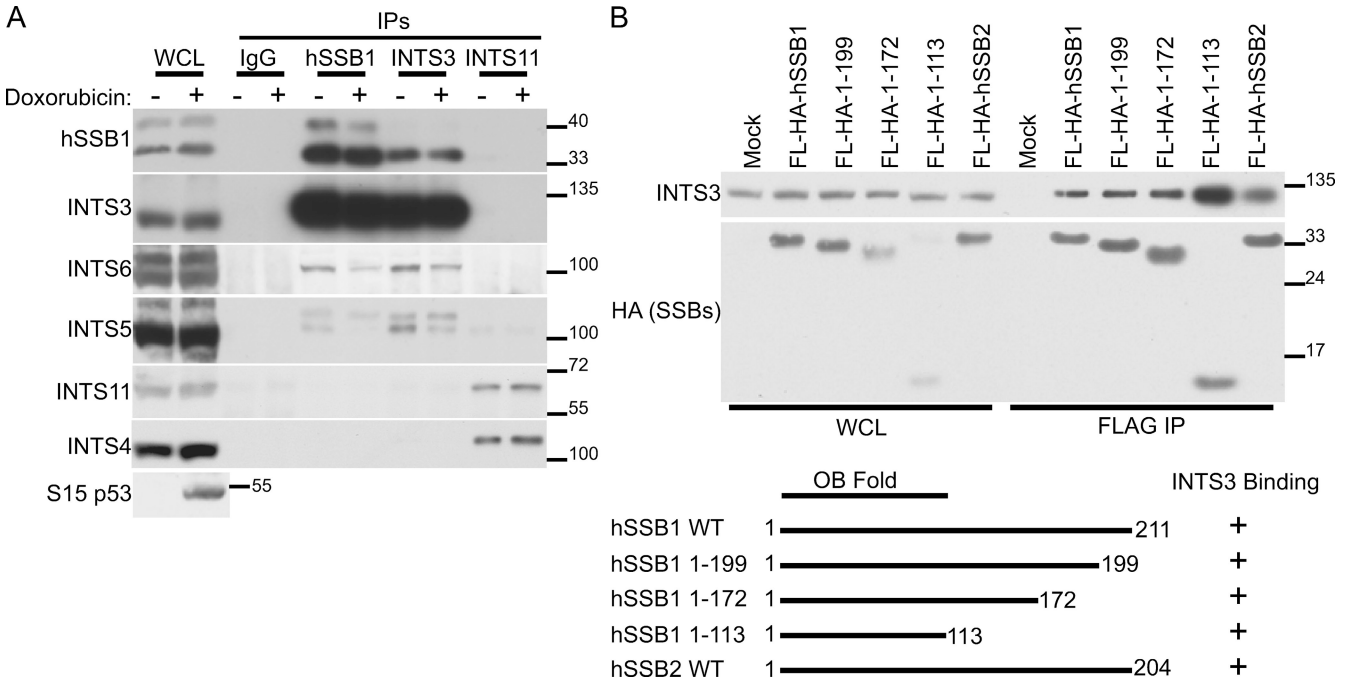

Figure 2. **INTS3–hSSB1 binding is independent of DNA damage and requires the hSSB1 OB fold.** (A) NHFs were mock treated or treated with 2 µg/µl doxorubicin for 1.5 h before harvesting by sonication in lysis buffer containing benzonase. Lysates were immunoprecipitated for the indicated proteins, separated by SDS-PAGE, and Western blotted as indicated. (B) HEK293T cells were mock transfected or transfected with the following Flag-HA–tagged constructs: hSSB1, hSSB1 1–199, hSSB1 1–172, hSSB1 1–113, or hSSB2. 48 h after transfection, cells were harvested, and lysates were immunoprecipitated with anti-Flag (FL) M2 agarose, separated by SDS-PAGE, and Western blotted as indicated. Flag-HA-hSSB2–transfected samples were treated with 2 µg/µl doxorubicin 1 h before harvesting. (A and B) Molecular mass is indicated in kilodaltons. IP, immunoprecipitation; WCL, whole cell lysate; WT, wild type.

To investigate this complex, immunoprecipitations of endogenous hSSB1 and INTS3 and -11 were performed from a variety of cell types (Figs. 1 C and 2 A and not depicted). In accordance with the MudPIT NSAF values, endogenous hSSB1 and INTS3 coimmunoprecipitated each other, while coimmunoprecipitating smaller amounts of INTS6, -5, and -1. (INTS3 binds the faster-migrating and most abundant band detected by hSSB1 antibodies; hSSB1 knockdown suggests that the slower-migrating band is nonspecific or a splice variant that is insensitive to the siRNA [Fig. S1 A].) Notably, neither hSSB1 nor INTS3 displayed binding to INTS11, and, unlike hSSB1 and INTS3, INTS11 coimmunoprecipitated INTS4, a member of the Integrator complex which was not detected in hSSB1 MudPIT samples. The failure of INTS3 and -11 to coimmunoprecipitate each other may result from the bulk of INTS3 being sequestered in IMS1 instead of binding the Integrator complex, or it may reflect substoichiometric association of INTS3 with the Integrator complex. These data demonstrate that hSSB1 forms a complex with INTS3 and smaller amounts of ancillary Integrator subunit proteins, including INTS6, -5, and -1; alternatively, INTS6, -5, -8, and -1 may be only weakly associated with the core complex and lost during immunoprecipitation and washing. Overall, the IMS1 complex appears distinct from the previously reported RNA polymerase II–associated complex carrying INTS11 catalytic activity (Baillat et al., 2005).

The presence of an additional, uncharacterized protein in the MudPIT analysis also suggested that the IMS1 complex is unique. To confirm the binding of MISE to hSSB1 and INTS3, Myc-tagged MISE was expressed in HEK293T cells, and immunoprecipitations were performed for hSSB1, INTS3, and the Myc tag (Fig. 1 D). Myc-MISE reciprocally coimmunoprecipitated with both hSSB1 and INTS3. The relatively small amount of Myc-MISE coimmunoprecipitating with hSSB1 and INTS3 is likely caused by the requirement of Myc-MISE to displace endogenous MISE. In conjunction with the NSAF data, which show that hSSB1 complexes contain 20 times more MISE than the ancillary INTS proteins, this result supports the conclusion that the core of this unique complex contains hSSB1, INTS3, and MISE.

IMS1 complex formation is independent of DNA damage

Because hSSB1 functions in the DNA damage response, the regulation of the IMS1 complex by DNA damage was investigated. Normal human fibroblasts (NHFs) were treated with doxorubicin before harvesting and immunoprecipitation for endogenous hSSB1 and INTS3 and -11 (Fig. 2 A). As predicted by the binding of both the T117A and T117E mutants to INTS3, hSSB1 and INTS3 were reciprocally coimmunoprecipitated in the presence or absence of DNA damage. The INTS3–hSSB1 interaction was insensitive to sonication and benzonase treatment, making it unlikely to be mediated through DNA or RNA. Similar to the results from U-2 OS cells (Fig. 1 C), both hSSB1 and INTS3 bound lesser amounts of INTS6 and INTS5 and did not bind INTS4 (Fig. 2 A). INTS11 failed to coimmunoprecipitate with either hSSB1 or INTS3 under either condition, although it coimmunoprecipitated INTS4.

The interaction of INTS3 and hSSB1 is independent of DNA damage and Thr117 phosphorylation, so we explored the interaction via INTS3 and hSSB1 truncation mutants. INTS3

Published September 28, 2009

deletion mutants were expressed in HEK293T cells, and immunoprecipitates were blotted for endogenous hSSB1 (Fig. S1 B). Although INTS3 mutants 1–675 and 1–512, containing an intact DUF2356 domain (PFAM domain of unknown function 2356; Finn et al., 2008), were capable of coimmunoprecipitating hSSB1, truncations disrupting all or part of the domain were unable to bind hSSB1. Notably, this domain is strictly conserved in INTS3 orthologues.

In the reciprocal experiment, immunoprecipitation of hSSB1 deletion mutants determined that the OB fold domain is sufficient for INTS3 binding, as hSSB1 1–113, containing only the OB fold, bound endogenous INTS3 (Fig. 2 B). The OB fold domains of hSSB1 and hSSB2 (an uncharacterized hSSB1 paralogue) are highly identical (>85%; Richard et al., 2008), and, as such, hSSB2 also bound INTS3 (Fig. 2 B, last lane), suggesting that INTS3 and hSSB2 may form an analogous IMS2 complex. Because the OB fold domain mediates hSSB1 binding to DNA, these results imply that INTS3 may impede the binding of hSSB1 to DNA, potentially regulating the relocalization of hSSB1 to foci after genotoxic stress. This result also suggests that INTS3 may not relocalize with hSSB1 to these foci. Finally, the strict conservation of the hSSB1 OB fold and the INTS3 DUF2356 further strengthens the notion that INTS3 binding is important for controlling the functions of hSSB1.

INTS3 controls the hSSB1-mediated response to DNA damage

Many DNA damage response and repair proteins rapidly relocalize to damaged DNA after genotoxic stress, forming discreet foci. Like other ATM pathway proteins, after DNA damage, hSSB1 rapidly relocalizes to sites of DNA damage (Richard et al., 2008). Although in analyses by immunoprecipitation and Western blotting the formation of the IMS1 complex appears unaffected by DNA damage, it was unknown whether INTS3 and MISE play a role in the DNA damage–related functions of hSSB1. Therefore, the potential of INTS3 to form DNA damage foci, colocalizing with hSSB1 and other DNA damage response proteins, was investigated. In unextracted cells, endogenous INTS3 exhibited pan nuclear staining (not depicted), but after Triton X-100 extraction of nonchromatin-bound proteins, INTS3 exhibited staining in discreet foci (Fig. S2). However, these foci were not DNA damage inducible and did not colocalize with either hSSB1 or γ-H2AX at damage-induced foci (Fig. S2, A and B), which form within minutes after DNA damage. At extended time points after irradiation (4 h), INTS3 did display a high degree of colocalization with γ-H2AX (Fig. S2 C), but the significance of relocalization at such a late time is unclear. INTS3 also did not localize to a single double-strand break induced by I-SceI expression (Fig. S2 D; Pierce et al., 1999). These results are consistent with the binding of INTS3 to the OB fold of hSSB1, which may block the ability of hSSB1 to bind DNA, suggesting a potential role for the IMS1 complex in regulating the recruitment of hSSB1 to DNA after DNA damage. Such a role would also be consistent with the DNA damage–independent formation of the IMS1 complex; even after relocalization of a population of hSSB1 to foci, the complex could form with any available free hSSB1 that is either newly synthesized or not recruited to DNA. Alternatively, similar to CHK2, INTS3 may be recruited transiently to irradiation-induced foci, making immediate detection difficult (Lukas et al., 2003), but the unrepaired/difficult to repair sites observed at late time points could stabilize this transient interaction, allowing detection of INTS3 at these sites (Goodarzi et al., 2008). Additionally, hSSB1 could exist in two forms, one form (which does not bind INTS3) that is able to relocalize to foci and a second form that constitutively binds INTS3. Finally, it remains possible that MISE but not INTS3 is capable of relocalizing to sites of DNA damage with hSSB1.

To investigate the role of IMS1 in controlling hSSB1 function, the DNA damage–induced localization of hSSB1 was examined after INTS3 knockdown by siRNA in NHFs (Fig. 3 A). Upon INTS3 knockdown, >75% of the cells examined failed to form hSSB1 foci after irradiation, demonstrating a role for IMS1 in controlling hSSB1. This defect appears to reflect a depletion of hSSB1 levels, with a consequent deficiency in hSSB1 recruitment to DNA damage sites (Fig. 3, A, C, and D). The ability of RAD51, a key component of the HR machinery, to form foci can be used as an indicator of DNA repair by HR, and hSSB1 has been shown to affect RAD51 foci formation (Richard et al., 2008). To confirm that the observed effect on hSSB1 levels results in inhibition of the DNA damage response, the ability of RAD51 to localize to DNA damage–induced foci was examined after INTS3 knockdown. Consistent with the depletion of hSSB1, INTS3 knockdown cells exhibited severe defects in the recruitment of RAD51 to DNA damage foci, with a 3.5-fold decrease in cells displaying RAD51 foci (Fig. 3 B). These results show that INTS3 regulates the recruitment of RAD51 to DNA breaks.

The effect of INTS3 depletion on hSSB1 and RAD51 DNA damage–induced foci suggested that IMS1 could control the global response to DNA damage. Previously, hSSB1 was demonstrated to act as an upstream effector for ATM activation (Richard et al., 2008). To test whether IMS1 is required for ATM activation after DNA damage, NHFs were transfected with siRNAs targeting INTS3 and MISE and were subjected to either irradiation or doxorubicin treatment (Fig. 3, C and D). In control siRNA–transfected cells, the response to DNA damage appeared normal, as assessed by ATM autophosphorylation and phosphorylation of downstream targets such as CHK2 and p53. In contrast, INTS3 or MISE knockdown cells displayed a dramatic decrease in ATM activation, with lower levels of CHK2 and p53 phosphorylation, which correlated with the degree of INTS3 or MISE depletion, indicating that IMS1 complex components are required for ATM activation. Moreover, INTS3 depletion affected ATM activation at early and late time points after irradiation (Fig. S3 A). Importantly, ATM and CHK2 activation was unaffected by INTS11 knockdown, further suggesting that the IMS1 complex functions independently of the Integrator complex (Fig. S3 B).

INTS3 regulates the transcription of hSSB1

Depletion of INTS3 by siRNA results in decreased levels of hSSB1 (Fig. 3, C and D). In the absence of genotoxic stress, hSSB1 is relatively unstable (Richard et al., 2008), and the ability to codeplete INTS3 and hSSB1 suggested that the IMS1

Published September 28, 2009

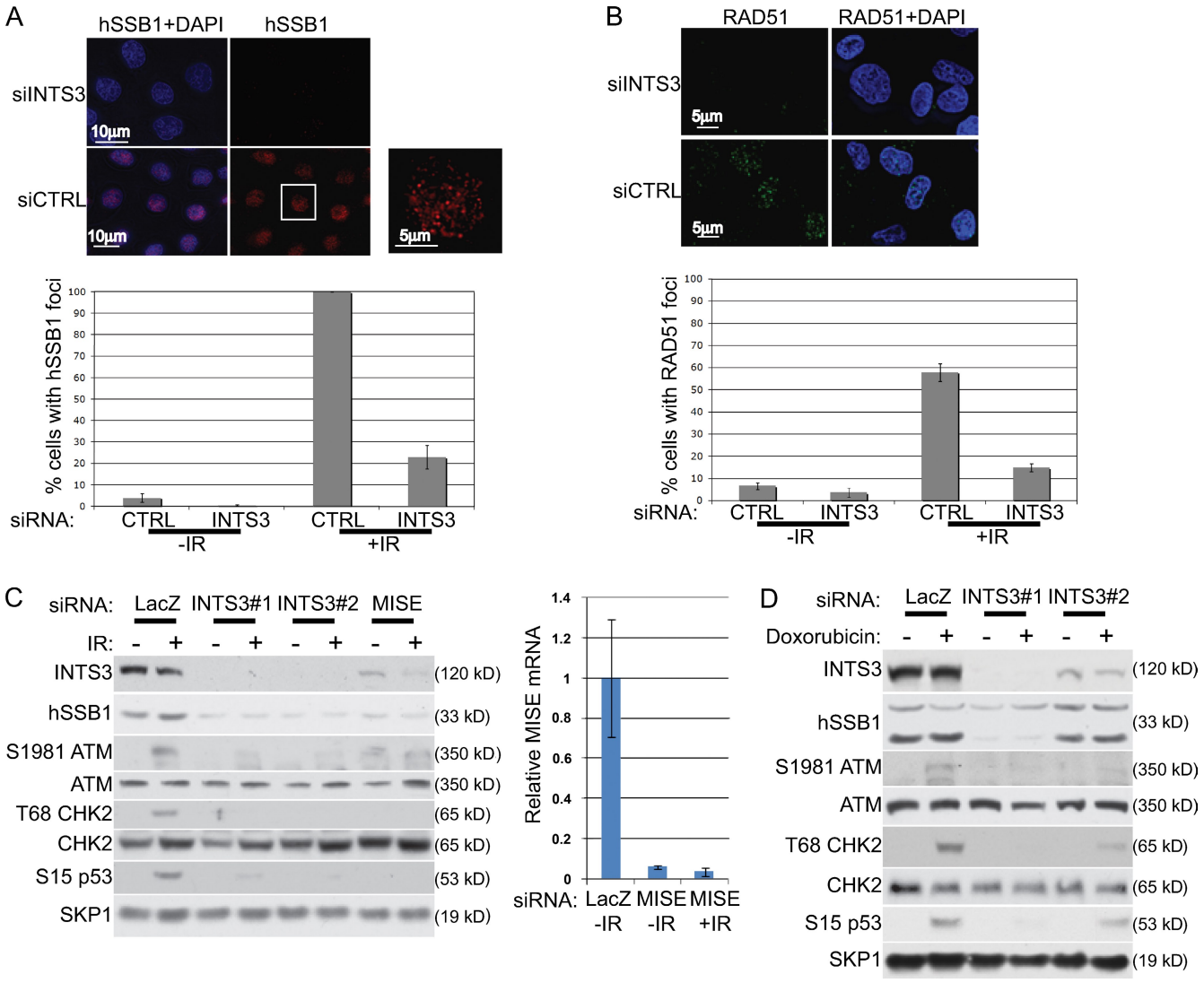

Figure 3. **INTS3 depletion blocks the hSSB1-mediated DNA damage response.** (A) NHFs were transfected with a control (CTRL) siRNA or INTS3 siRNA #1 before irradiation (6 Gy) and recovered for 1 h before staining for hSSB1 and DAPI. The top panel presents a representative field of ionizing radiation (IR)–treated cells, and the bottom panel shows the quantification of total results presented as mean ± SEM from three independent experiments. The inset shows a single cell enlarged. (B) NHFs were transfected with a control siRNA or INTS3 siRNA #1 before irradiation (6 Gy) and recovered for 3 h before staining for RAD51 and DAPI. The top panel presents a representative field of RAD51 foci in ionizing radiation–treated cells (deconvolved), and the bottom panel shows the quantification of total results presented as mean ± SEM from three independent experiments. (C) NHFs were transfected twice with the indicated siRNAs. 72 h after transfection, cells were irradiated (7.5 Gy) and harvested 1 h after irradiation. Lysates were analyzed by SDS-PAGE and Western blotting (left) as indicated. Evaluation of MISE knockdown was performed using RT-PCR in triplicate (right). The mean values are shown plus or minus one standard deviation. (D) NHFs were transfected twice with the indicated siRNAs. 72 h after transfection, cells were treated with 2 µg/ml doxorubicin for 1.5 h and harvested. Lysates were analyzed by SDS-PAGE and Western blotting as indicated.

complex may preserve a pool of hSSB1 from degradation in the absence of DNA damage to allow rapid activation of the DNA damage response. To test this hypothesis, hSSB1 stability was measured by determining its half-life in cycloheximide after INTS3 knockdown. In contrast to the predicted results, INTS3 knockdown severely reduced the level of hSSB1 without decreasing the half-life of hSSB1 (Fig. 4 A).

Because the effect of INTS3 knockdown on hSSB1 appeared largely degradation independent, the impact of INTS3 on hSSB1 mRNA levels was examined (Fig. 4 B). Strikingly, INTS3 knockdown decreased hSSB1 mRNA levels by 90% versus control knockdown, demonstrating that INTS3 likely controls hSSB1 transcription. To investigate this hypothesis, the ability of a constitutive promoter to uncouple hSSB1 from INTS3-based regulation was examined (Fig. 4, C and D; and Fig. S3, C and D). In cells expressing near-endogenous levels of hSSB1 from a retrovirus, INTS3 depletion failed to deplete exogenous hSSB1 or abrogate hSSB1 foci formation, confirming that the observed defects in hSSB1 levels and foci result from a defect in hSSB1 transcription. Furthermore, retrovirally expressed hSSB1 rescued RAD51 foci formation in INTS3-depleted cells, demonstrating that the effect of INTS3 on RAD51 foci is hSSB1 dependent (Fig. 4 E).

Our results demonstrate the existence of an IMS1 complex, featuring a core of INTS3, MISE, and hSSB1 (or possibly hSSB2 in an IMS2 complex), with ancillary Integrator subunits

Published September 28, 2009

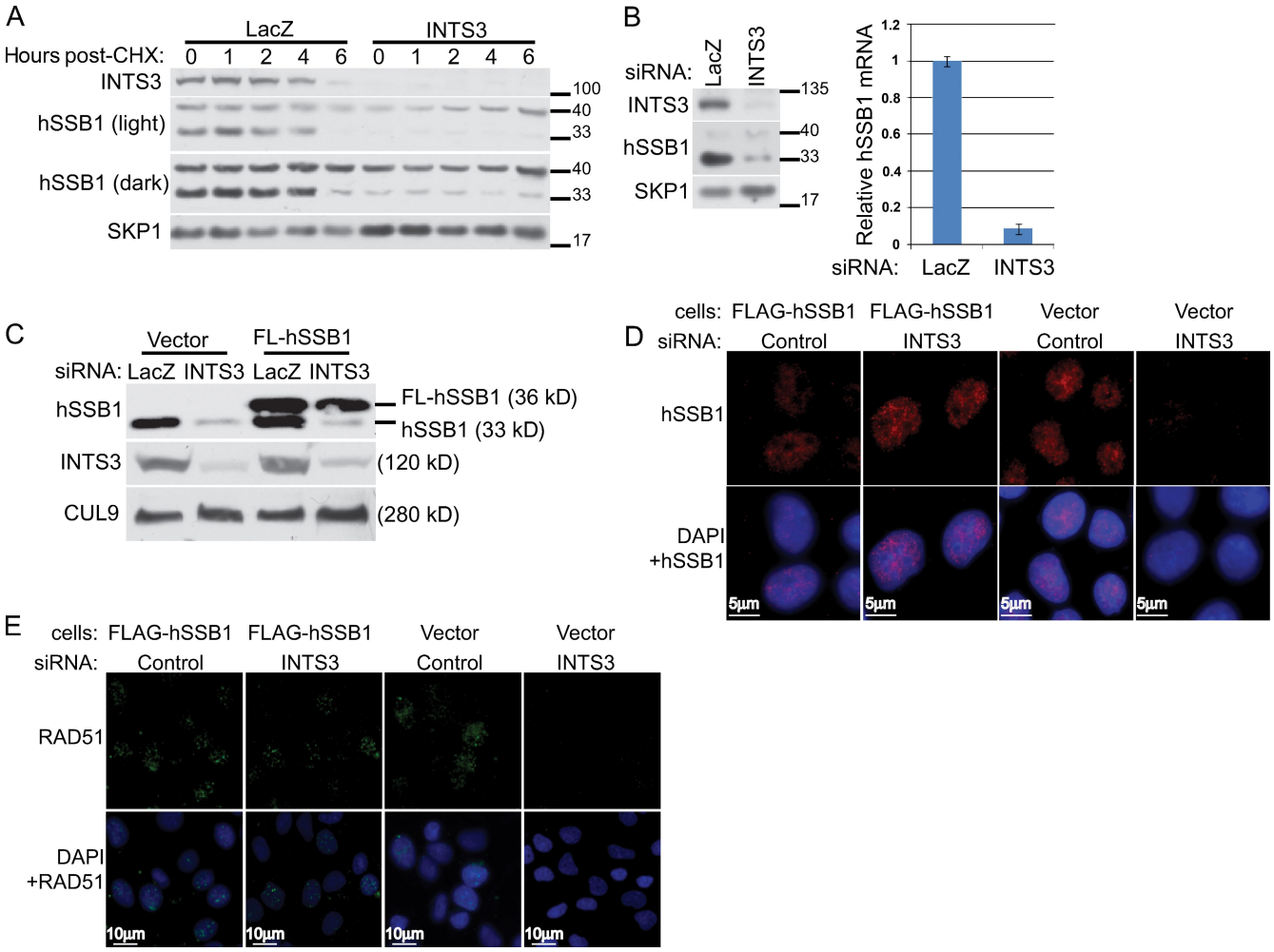

Figure 4. **INTS3 controls hSSB1 transcription.** (A) NHFs were transfected twice with the indicated siRNAs. 72 h after transfection, cells were treated with cycloheximide (CHX) for the indicated time period. Lysates were analyzed by SDS-PAGE and Western blotting as indicated. (B) NHFs were transfected twice with the indicated siRNAs. 72 h after transfection, cells were harvested for preparation of mRNA and protein lysates. Western blotting was performed as indicated (left). RT-PCR for hSSB1 was performed in triplicate and is presented as the mean plus or minus one standard deviation (right). (A and B) Molecular mass is indicated in kilodaltons. (C) HEK293T cells stably expressing Flag (FL)-hSSB1 from a retroviral vector or HEK293T cells infected with an empty vector were transfected with LacZ siRNA or INTS3 siRNA #1 as indicated. 72 h after transfection, lysates were generated and analyzed by SDS-PAGE and Western blotting. Exogenous Flag-hSSB1 and endogenous hSSB1 are indicated. (D) MCF7 cells stably expressing Flag-hSSB1 from a retroviral vector or MCF7 cells infected with an empty vector were transfected with a control siRNA or INTS3 siRNA #1 before irradiation (6 Gy) and recovered for 1 h before staining for hSSB1 and DAPI. (E) MCF7 cells stably expressing Flag-hSSB1 from a retroviral vector or MCF7 cells infected with an empty vector were transfected with a control siRNA or INTS3 siRNA #1 before irradiation (6 Gy) and recovered for 1 h before staining for RAD51 and DAPI.

binding in a substoichiometric manner. IMS1 assembly is not regulated by ATM activation after DNA damage, suggesting that the ancillary members or other weak/transient interacting proteins may regulate the core complex's role in the DNA damage response. The role of these ancillary INTS proteins in the DNA damage response will require further examination.

Remarkably, in addition to binding hSSB1, INTS3 regulates the abundance of hSSB1 at the transcriptional level. The formation of IMS1 coupled with this transcriptional regulation suggests the operation of a positive feedback loop in the DNA damage response. In such a model, INTS3 likely controls the cellular reserves of hSSB1 through the control of hSSB1 transcription and possibly via physical sequestration.

The INTS3–hSSB1 feedback loop establishes a new network in the control of the DNA damage response. Given the frequency of mutation of ATM and other DNA damage repair proteins in cancer and radiosensitivity syndromes, it is possible that pathogenic mutations in INTS3 or hSSB1 will be found. The IMS1 complex may also represent a target for chemotherapeutics that sensitize tumor cells to DNA-damaging treatments (Farmer et al., 2005). INTS3 is clearly required for an effective DNA damage response, and further research into additional targets, biochemical mechanisms, and potential roles in disease is required.

Materials and methods

Cell lines, transfection, and siRNAs

HEK293T cells were maintained in DME supplemented with 10% bovine serum (Invitrogen), and all other cells (U-2 OS, MCF7, MCF7 DR-GFP [gift from J. Jasin, Memorial Sloan-Kettering Cancer Center, New York, NY], and NHFs) were maintained in DME supplemented with 10% fetal bovine serum (Invitrogen). NHFs were either neonatal foreskin fibroblasts (immunofluorescence microscopy) or IMR90 (all other experiments). MCF7 and HEK293T cells stably expressing Flag-hSSB1 were

Published September 28, 2009

generated by retroviral infection. HEK293T cells were transfected using calcium phosphate, and siRNA transfections were performed with Metafectene Pro (Biontex) or Lipofectamine 2000 (Invitrogen). The following siRNAs were used: control, 5′-UUCUCCGAACGUGUCACGUAUUUAG-3′; LacZ, 5′-CGUACGCGGAAUACAACGA-3′; INTS3#1, 5′-GAUGAGAGUUGCUAUGACA-3′; INTS3#2, 5′-ACAACCAUAUGUCGGAUAA-3′; MISE#1, 5′-GAACCAGUCUUCAACAAAU-3′; MISE#2, 5′-AAAUAGAGUUGCAAUCUUG-3′; INTS11#1, 5′-UAACAGACUUCCUGGACUG-3′; INTS11#2, 5′-CAAGAUCGCCGUAGACAAG-3′; and hSSB1, 5′-GUUCGGACCUGCAAAGUGG-3′. For MISE knockdown, both oligonucleotides were used. Cells were doxorubicin (Sigma-Aldrich) treated as indicated using a 2 mg/ml stock in PBS.

Western blotting and antibodies

Normal rabbit IgG and rabbit polyclonal antibodies to INTS3, -11, -6, -5, and -4 and actin, Myc, hSSB1, CUL9, and HA were obtained from Bethyl Laboratories, Inc. Other rabbit antibodies used include hSSB1 (generated against bacterially expressed hSSB1), phospho-Ser15 p53 (Cell Signaling Technology), Skp1 (Santa Cruz Biotechnology, Inc.), ATM (Abcam), phospho-Thr68 CHK2 (Cell Signaling Technology), and CHK2 (Santa Cruz Biotechnology, Inc.). Mouse monoclonal antibodies used include phospho-Ser1981 ATM (Cell Signaling Technology), Myc (9B11; Cell Signaling Technology), and HA (12CA5). Cell lysates were generated in lysis buffer (50 mM Tris, pH 8.0, 250 mM NaCl, 1 mM EDTA, 50 mM NaF, and 0.5% Triton X-100) supplemented with protease and phosphatase inhibitors. Select samples were generated by sonication (Bioruptor; Diagenode) in lysis buffer containing 1 U/µl benzonase. Western blotting was performed as described previously (Skaar et al., 2007). The following additional antibodies were used for immunofluorescence microscopy: hSSB1 (sheep), RAD51 (mouse; EMD), γ-H2AX (mouse; Millipore), and HA (rabbit; Cell Signaling Technology). Half-life measurements were performed using 100 µg/ml cycloheximide.

Immunofluorescence microscopy

For immunofluorescence, cells were prepermeabilized with 20 mM Hepes, pH 8.0, 20 mM NaCl, 5 mM $MgCl_2$, 1 mM ATP, 0.1 mM N_2OV, 1 mM NaF, and 0.5% NP-40 for 15 min on ice before fixation in 4% paraformaldehyde (wt/vol) in PBS for 10 min. Cells were then treated for 10 min with 0.5% Triton X-100 before being blocked with 3% BSA in PBS for 30 min. Primary antibodies were incubated for 1 h, and secondary antibodies were incubated for 30 min at room temperature in 3% BSA PBS. All cells for immunofluorescence were cultured on 8-well microslides (Ibidi). Slides were prepared using Mowiol imaging media and secondary antibodies conjugated to either Alexa Fluor 488 or Alexa Fluor 594. Additionally, cells were stained with DAPI. Images were captured at room temperature using a 20-MHz camera (CoolSNAP ES2; Photometrics) linked to a microscope (PDV; Applied Precision, LLC) using either a 60× NA 1.42 or 100× NA 1.65 objective lens, as indicated. Images were acquired and analyzed with SoftWoRx 3.7.0 (Linux). Brightness and contrast were altered with SoftWoRx 3.7.0 to give optimal images for publication. All operations to one image were copied and pasted to the subsequent comparison images to allow comparison. Where images were deconvolved, this was performed using the SoftWoRx 3.7.0 software using the default additive deconvolution algorithm. Images were exported as a single image from a stack as a TIFF file. The TIFF file was opened in Photoshop CS3 (Adobe), where the images were all cropped (using the same area).

Cloning and RT-PCR

hSSB1, hSSB2, and MISE cDNAs were PCR amplified and cloned from HeLa cDNA into pcDNA 3.0 Flag-HA or pcDNA 3.0 Myc. The INTS3 cDNA was generated by PCR from IMAGE clone 5752962 (Thermo Fisher Scientific) and cloned into pcDNA 3.0 HA. All truncation mutants and point mutants were subsequently generated by PCR or QuikChange (Agilent Technologies), respectively. The cDNAs were verified by sequencing. cDNA was generated from total RNA (RNeasy; QIAGEN) using Superscript III (Invitrogen). RT-PCR was performed in triplicate using SYBR green (Bio-Rad Laboratories).

Tandem affinity purification and mass spectrometry

Tandem affinity purification was performed as previously described with the following modifications (Skaar et al., 2007). HEK293T cells were transiently transfected with Flag-HA constructs using calcium phosphate, and 48 h after transfection, whole cell extracts were generated in lysis buffer (50 mM Tris, pH 8.0, 250 mM NaCl, 1 mM EDTA, 50 mM NaF, and 0.5% Triton X-100) supplemented with protease and phosphatase inhibitors. Lysis buffer was used for all subsequent washes. MudPIT of TCA-precipitated proteins was performed as previously described (Washburn et al., 2001; MacCoss et al., 2002; Florens and Washburn, 2006). Tandem mass spectra were interpreted using SEQUEST (Eng et al., 1994) against a database of 61,430 sequences, consisting of 30,552 human proteins (NCBI Protein database on March 4, 2008), 177 usual contaminants, and, to estimate false discovery rates, 30,712 randomized amino acid sequences derived from each nonredundant protein entry. Peptide/spectrum matches were sorted and selected using DTASelect (Tabb et al., 2002) with the following criteria set: spectra/peptide matches were only retained if they had a DeltCn of at least 0.08 and minimum XCorr of 1.8 for singly, 2.5 for doubly, and 3.5 for triply charged spectra. Peptides had to be fully tryptic and at least 7 aa long, and positive identification required two unique peptides or one peptide with two independent spectra. The final false discovery rates at the protein and spectral levels were 1.9% and 0.14 ± 0.085%, respectively. NSAFs were calculated for each detected protein (Florens et al., 2006; Paoletti et al., 2006; Zybailov et al., 2006).

Online supplemental material

Fig. S1 shows that DUF2356 is required for INTS3 binding to hSSB1. Fig. S2 shows that INTS3 does not localize to irradiation-induced DNA damage sites. Fig. S3 shows that INTS3 but not INTS11 is required for proper ATM activation. Online supplemental material is available at http://www.jcb.org/cgi/content/full/jcb.200907026/DC1.

We thank E. McIntush (Bethyl Laboratories, Inc.) for antibodies, M. Jasin for MCF7 DR-GFP cells, and M.L. Skaar and C.M. Hughes for reading the manuscript. M. Pagano is grateful to T.M. Thor for continuous support.

This work was funded by grants from the National Health and Medical Research Council of Australia to K.K. Khanna and grants from the National Institutes of Health (R01-GM057587, R37-CA076584, and R21-CA125173) and the Multiple Myeloma Research Foundation to M. Pagano. M. Pagano is an Investigator with the Howard Hughes Medical Institute. J.R. Skaar is supported by the Mr. and Mrs. William G. Campbell Postdoctoral Fellowship in Memory of Carolyn Cabott from the American Cancer Society. A. Saraf, L. Florens, and M.P. Washburn are supported by the Stowers Institute for Medical Research.

Submitted: 6 July 2009
Accepted: 3 September 2009

References

Baillat, D., M.A. Hakimi, A.M. Näär, A. Shilatifard, N. Cooch, and R. Shiekhattar. 2005. Integrator, a multiprotein mediator of small nuclear RNA processing, associates with the C-terminal repeat of RNA polymerase II. *Cell*. 123:265–276. doi:10.1016/j.cell.2005.08.019

Buchmann, A.M., J.R. Skaar, and J.A. DeCaprio. 2004. Activation of a DNA damage checkpoint response in a TAF1-defective cell line. *Mol. Cell. Biol.* 24:5332–5339. doi:10.1128/MCB.24.12.5332-5339.2004

Derheimer, F.A., H.M. O'Hagan, H.M. Krueger, S. Hanasoge, M.T. Paulsen, and M. Ljungman. 2007. RPA and ATR link transcriptional stress to p53. *Proc. Natl. Acad. Sci. USA*. 104:12778–12783. doi:10.1073/pnas.0705317104

Dominski, Z., X.C. Yang, M. Purdy, E.J. Wagner, and W.F. Marzluff. 2005. A CPSF-73 homologue is required for cell cycle progression but not cell growth and interacts with a protein having features of CPSF-100. *Mol. Cell. Biol.* 25:1489–1500. doi:10.1128/MCB.25.4.1489-1500.2005

Eng, J.K., A.L. McCormack, and J.R. Yates III. 1994. An approach to correlate tandem mass spectral data of peptides with amino acid sequences in a protein database. *J. Am. Soc. Mass Spectrom.* 5:976–989. doi:10.1016/1044-0305(94)80016-2

Farmer, H., N. McCabe, C.J. Lord, A.N. Tutt, D.A. Johnson, T.B. Richardson, M. Santarosa, K.J. Dillon, I. Hickson, C. Knights, et al. 2005. Targeting the DNA repair defect in BRCA mutant cells as a therapeutic strategy. *Nature*. 434:917–921. doi:10.1038/nature03445

Finn, R.D., J. Tate, J. Mistry, P.C. Coggill, S.J. Sammut, H.R. Hotz, G. Ceric, K. Forslund, S.R. Eddy, E.L. Sonnhammer, and A. Bateman. 2008. The Pfam protein families database. *Nucleic Acids Res.* 36:D281–D288. doi:10.1093/nar/gkm960

Florens, L., and M.P. Washburn. 2006. Proteomic analysis by multidimensional protein identification technology. *Methods Mol. Biol.* 328:159–175.

Florens, L., M.J. Carozza, S.K. Swanson, M. Fournier, M.K. Coleman, J.L. Workman, and M.P. Washburn. 2006. Analyzing chromatin remodeling complexes using shotgun proteomics and normalized spectral abundance factors. *Methods*. 40:303–311. doi:10.1016/j.ymeth.2006.07.028

Goodarzi, A.A., A.T. Noon, D. Deckbar, Y. Ziv, Y. Shiloh, M. Löbrich, and P.A. Jeggo. 2008. ATM signaling facilitates repair of DNA double-strand breaks associated with heterochromatin. *Mol. Cell*. 31:167–177. doi:10.1016/j.molcel.2008.05.017

Hata, T., and M. Nakayama. 2007. Targeted disruption of the murine large nuclear KIAA1440/Ints1 protein causes growth arrest in early blastocyst stage embryos and eventual apoptotic cell death. *Biochim. Biophys. Acta*. 1773:1039–1051. doi:10.1016/j.bbamcr.2007.04.010

Kang, H.S., J.Y. Beak, Y.S. Kim, R.M. Petrovich, J.B. Collins, S.F. Grissom, and A.M. Jetten. 2006. NABP1, a novel RORgamma-regulated gene encoding a single-stranded nucleic-acid-binding protein. *Biochem. J.* 397:89–99. doi:10.1042/BJ20051781

Lainé, J.P., and J.M. Egly. 2006. When transcription and repair meet: a complex system. *Trends Genet.* 22:430–436. doi:10.1016/j.tig.2006.06.006

Lavin, M.F. 2007. ATM and the Mre11 complex combine to recognize and signal DNA double-strand breaks. *Oncogene*. 26:7749–7758. doi:10.1038/sj.onc.1210880

Lukas, C., J. Falck, J. Bartkova, J. Bartek, and J. Lukas. 2003. Distinct spatio-temporal dynamics of mammalian checkpoint regulators induced by DNA damage. *Nat. Cell Biol.* 5:255–260. doi:10.1038/ncb945

MacCoss, M.J., W.H. McDonald, A. Saraf, R. Sadygov, J.M. Clark, J.J. Tasto, K.L. Gould, D. Wolters, M. Washburn, A. Weiss, et al. 2002. Shotgun identification of protein modifications from protein complexes and lens tissue. *Proc. Natl. Acad. Sci. USA*. 99:7900–7905. doi:10.1073/pnas.122231399

Nakatani, Y., and V. Ogryzko. 2003. Immunoaffinity purification of mammalian protein complexes. *Methods Enzymol.* 370:430–444. doi:10.1016/S0076-6879(03)70037-8

Paoletti, A.C., T.J. Parmely, C. Tomomori-Sato, S. Sato, D. Zhu, R.C. Conaway, J.W. Conaway, L. Florens, and M.P. Washburn. 2006. Quantitative proteomic analysis of distinct mammalian Mediator complexes using normalized spectral abundance factors. *Proc. Natl. Acad. Sci. USA*. 103:18928–18933. doi:10.1073/pnas.0606379103

Pierce, A.J., R.D. Johnson, L.H. Thompson, and M. Jasin. 1999. XRCC3 promotes homology-directed repair of DNA damage in mammalian cells. *Genes Dev.* 13:2633–2638. doi:10.1101/gad.13.20.2633

Richard, D.J., E. Bolderson, L. Cubeddu, R.I. Wadsworth, K. Savage, G.G. Sharma, M.L. Nicolette, S. Tsvetanov, M.J. McIlwraith, R.K. Pandita, et al. 2008. Single-stranded DNA-binding protein hSSB1 is critical for genomic stability. *Nature*. 453:677–681. doi:10.1038/nature06883

Skaar, J.R., L. Florens, T. Tsutsumi, T. Arai, A. Tron, S.K. Swanson, M.P. Washburn, and J.A. DeCaprio. 2007. PARC and CUL7 form atypical cullin RING ligase complexes. *Cancer Res.* 67:2006–2014. doi:10.1158/0008-5472.CAN-06-3241

Tabb, D.L., W.H. McDonald, and J.R. Yates III. 2002. DTASelect and Contrast: tools for assembling and comparing protein identifications from shotgun proteomics. *J. Proteome Res.* 1:21–26. doi:10.1021/pr015504q

Tao, S., Y. Cai, and K. Sampath. 2009. The Integrator subunits function in hematopoiesis by modulating Smad/BMP signaling. *Development*. 136:2757–2765. doi:10.1242/dev.034959

Washburn, M.P., D. Wolters, and J.R. Yates III. 2001. Large-scale analysis of the yeast proteome by multidimensional protein identification technology. *Nat. Biotechnol.* 19:242–247. doi:10.1038/85686

Wieland, I., K.C. Arden, D. Michels, L. Klein-Hitpass, M. Böhm, C.S. Viars, and U.H. Weidle. 1999. Isolation of DICE1: a gene frequently affected by LOH and downregulated in lung carcinomas. *Oncogene*. 18:4530–4537. doi:10.1038/sj.onc.1202806

Zybailov, B., A.L. Mosley, M.E. Sardiu, M.K. Coleman, L. Florens, and M.P. Washburn. 2006. Statistical analysis of membrane proteome expression changes in *Saccharomyces cerevisiae*. *J. Proteome Res.* 5:2339–2347. doi:10.1021/pr060161n

Zybailov, B.L., L. Florens, and M.P. Washburn. 2007. Quantitative shotgun proteomics using a protease with broad specificity and normalized spectral abundance factors. *Mol. Biosyst.* 3:354–360. doi:10.1039/b701483j